Journal of Physics: Conference Series

Vortex filament method 3D analysis of design parameters for counter-rotating axis floating tilted turbine

Vortex filament method 3D analysis of design parameters for counter-rotating axis floating tilted turbine

E Andersson[1], H Bernhoff[1,2] and A Goude[1]

[1] Dept. of Engineering Sciences, Division of Electricity, Uppsala University, Sweden
[2] World Wide Wind Tech AS, CTO, Norge

E-mail: emil.l.andersson@angstrom.uu.se, hans.bernhoff@angstrom.uu.se, anders.goude@angstrom.uu.se

Abstract.

The Counter-Rotating Axis Floating Tilted turbine (CRAFT) is a new design for floating off-shore wind power, which utilizes a low center of gravity and allows the tower to tilt to mitigate costs for platforming.

In this study, 3D simulations of the CRAFT have been performed to investigate the effect from the tower's tilt angle on the aerodynamics of the turbine using a vortex filament method. Due to lack of empirical data of the CRAFT, the method has been benchmark tested against a previous project on a vertical axis wind turbine.

Using this method, the blades' twist angle has been set to achieve good lift-to-drag ratio along the entire blade. Furthermore, the blades' chord length has been determined for optimal Tip Speed Ratio (TSR) 6 when the tower is tilted 30 degrees from vertical position.

The CRAFT has been simulated vertically and tilted 15°, 30° and 45°, for TSRs ranging between 4 and 9. The power coefficients (C_P) and normal forces have been determined, and velocity plots are presented to show how the near-wake develops.

The results from this study serves as a basis for further development and design of the CRAFT.

1. Introduction

There is currently a large interest in development of off-shore wind power[1, 2, 3]. Both vertical axis wind turbines (VAWTs) and horizontal axis wind turbines (HAWTs) have originally been developed for on-shore wind power and the concepts are not trivial to bring off-shore. The conditions for floating off-shore wind power prove new challenges[4, 5] and there is a large incentive to develop cost-effective alternatives.

The Counter-Rotating Axis Floating Tilted turbine (CRAFT), illustrated in figure 1, is a new design to mitigate platforming costs for floating off-shore wind power. The CRAFT consists of two counter-rotating turbines and is allowed to tilt with the wind, pivoting around a floater at the water's surface. To maintain the desired tower tilt angle during wind load, the generator and additional ballast are located underneath the water's surface. The CRAFT has potential to become a cost effective alternative for floating off-shore wind power, due to its low platform costs.

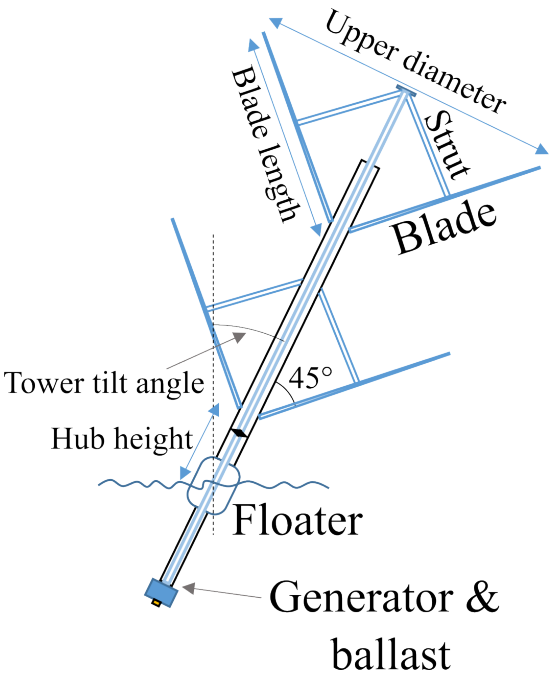

Figure 1: Geometry of CRAFT.

It is of great interest to study turbine performance and the wind loads on the blades when designing and developing new wind turbines. The CRAFT is unique from an aerodynamic perspective due to its two counter-rotating turbines and operation while tilting. Therefore, the effect of the tower's tilt angle on the performance and wind loads has been chosen as the main focus of this study.

2. Turbine design

The main geometry parameters are summarized in table 1. The CRAFT has been designed by the company World Wide Winds AS, Oslo[6], and is designed to operate for tilt angles between 0° and 45°. It is therefore effectively a combination of both a horizontal and vertical axis wind turbine.

The CRAFT, shown in figure 1, has two counter-rotating turbines, which in this study have similar geometry. The turbines are located at hub height 45 m and 110 m, and each turbine has an upper diameter of $D_U = 129$ m. Both turbines consist of three blades forming a V-shape, attached to the tower at the base and extending outwards and upwards at a 45° angle. The rotor sweeps a cone-shape and the swept 2D area of the rotor changes with the tower angle. The swept areas used for this work were numerically calculated, displayed in table 1. Struts are used to stabilize the blades and both the blades and struts have the cross-section of a NACA0021 wing profile. The NACA0021 wing profile has been chosen due to the availability of empirical data necessary for the simulation method described in section 3 and is not part of the final design of the CRAFT.

The turbine is illustrated in top-down view in figure 2. The rotational velocity and the azimuthal angle are denoted Ω and θ, respectively. The free stream velocity is denoted U_∞ and the relative wind velocity V_{rel} experienced by the blade is calculated from the free stream velocity and the rotational velocity of the blade. The free stream velocity is around 11 m/s on site[7]. The tip speed ratio (TSR) is defined as TSR $= R\Omega/U_\infty$. The rated TSR for the CRAFT is set to 6 to minimize the risk of leading edge erosion[8]. The normal and tangential forces, F_N and F_T in figure 2, are defined as positive in outward radial direction and in rotational direction, respectively.

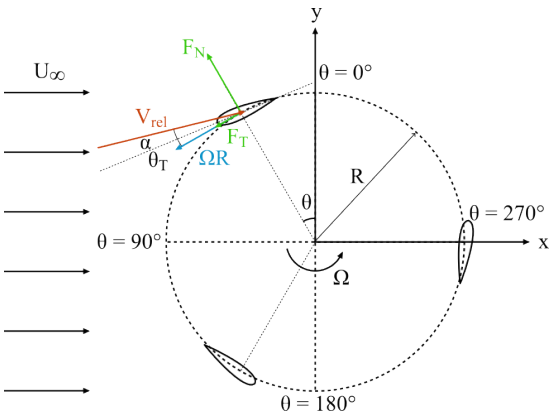

Figure 2: Azimuthal coordinates of rotational plane.

The blades have a twist angle, θ_T in figure 2, to ensure optimal angle of attack α along the full length of the blade. Optimal lift-to-drag ratio occur for angles of attack between 10°–15° for NACA0021[9]. To find the optimal twist angle, the vortex filament method described in section 3 was used to simulate the CRAFT for different tilt angles at TSR 6 and angle of attack was plotted. The twist angle along the blade was adjusted such that the peak angle of attack was between 10°–15° over a full revolution. The optimal twist angle starts at 15° at the base and increases to 19° at 3.6 m spanwise along the blade. The twist then gradually decreases to −5° at the tip.

The chord length affects the C_P-curve[10]. By varying the chord in simulations of the CRAFT using the vortex filament method described in section 3 and observing the shift in C_P-curve, the chord could be adjusted such that the peak for C_P occurred for TSR 6 for tower tilt angle 30°. The blades are tapered and have a chord length that goes from 8.4 m at the base to 1.8 m at the tip.

Table 1: Parameters of CRAFT. The swept area is for each of the rotors of the turbine.

Property	Value
Number of blades per turbine	3
Upper diameter	129 m
Tower diameter	28 m
Hub height 1	45 m
Hub height 2	110 m
Blade length	72 m
Blade/strut profile	NACA0021
Swept area for 0° tower angle	$4.0 \cdot 10^3$ m^2
Swept area for 15° tower angle	$5.6 \cdot 10^3$ m^2
Swept area for 30° tower angle	$7.1 \cdot 10^3$ m^2
Swept area for 45° tower angle	$9.3 \cdot 10^3$ m^2

3. Vortex filament method

The motion of fluid parcels in a fluid flow is described using the Navier-Stokes equation together with the continuity equation. Alternatively, vortex methods use the vortex formulation of Navier-Stokes, referred to as the vorticity equation. The vorticity equation is obtained by taking

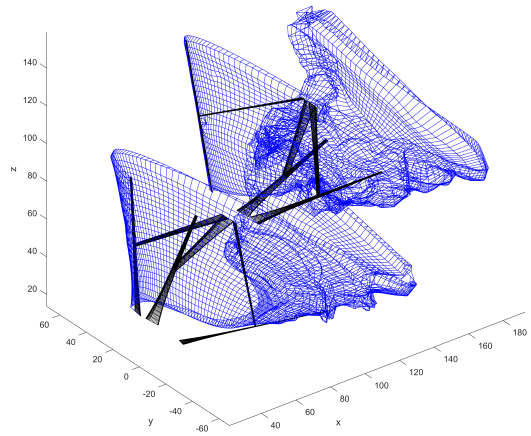

Figure 3: Example of vortex filament lattice released from one blade on each of the turbines of the CRAFT. For visual clarity, only a small part of the vortex filament wake is shown. The black lines represent the vortex panels used to solve the potential flow problem.

the curl of the Navier-Stokes equation and instead describes the motion of vorticity parcels in fluid flow.

It is more common for vortex methods to use a Lagrangian or "free vortex" description rather than Eulerian. In other words, the current method considers discrete vortices that are propagated with the flow. The velocity field is found from the potential flow solution and the contribution from the vortices by applying the Biot-Savart law[11]. The vortices are smoothed using a Rankine kernel smoothing function to avoid singularities. The size of the Rankine kernels is chosen each time step as 1.2 times the distance to the current nearest neighbour in the filament lattice to create an overlap.

Using free vortices is advantageous because it saves computational time by only requiring calculation particles for the vortices and a mesh-free domain. Here, a simulation domain that is infinitely large in the x and y direction is assumed, the only sources of vorticity being the turbine and the wake. Additionally, to simulate an impermeable ground, a method of images has been implemented. Each vortex created by the CRAFT is mirrored over the $(z = 0)$-plane by a vortex of equal and opposite vorticity. Thus, the regions with vorticity are the turbine, the wake, and the mirror image.

The implemented vortex method is a vortex *filament* method, meaning that the flow is approximated as discrete filaments or tubes of fluid[11]. The vortex filaments are constructed by line elements that form a lattice connected at grid points, illustrated in figure 3. Each blade and strut will generate a vortex filament lattice, describing its contribution to the flow field. The flow propagates the vortices by propagating the grid points with the fluid velocity at the grid point positions, $\frac{d(r_i)}{dt} = V(r_i)$.

To correctly handle the flow curvature and connection between strut and blade, the vortex method is combined with a panel method. Linear rectangular panels are used to model the turbine blades. Each blade and strut is constructed by rectangular panels divided into multiple segments. The the blade segments' bound circulation is determined by enforcing an impermeability condition on the surface of the airfoil and a Kutta condition on the trailing edge. The bound circulation of the blade Γ_{blade} is used to find the angle of attack for the blade, using the "explicit method" described in previous work by Dyachuck[12].

The angle of attack and the local Reynolds number are used to determine the lift and drag coefficients, C_L and C_D. These are then used together with the angle of attack and relative wind velocity to determine the lift and drag forces given by

$$F_L = \frac{1}{2}\rho c C_L |V_{rel}|^2, \tag{1}$$

$$F_D = \frac{1}{2}\rho c C_D |V_{rel}|^2, \tag{2}$$

where ρ is the air density and c is the chord length. However, the Kutta condition is used for ideal flow without stall, and a dynamic stall model has therefore been implemented to adjust the blade forces for cases with stall[13]. With the forces determined, the effective bound circulation can be calculated from the lift coefficient using the Kutta-Joukowski lift formula

$$\Gamma = \frac{1}{2} C_L c |V_{rel}|. \tag{3}$$

In the simulation, a vortex is released from the blade every time step such that the total circulation of the blade and the vortex is conserved between each time step.

The vortex filament method follows the following procedure for each time step:

(i) Use the panel method to calculate the potential flow circulation and evaluate the relative flow velocity at the quarter chord position for each blade segment.
(ii) Use the circulation to calculate the angle of attack from an empirical data table.
(iii) Use an external force model to determine the lift and drag forces on each blade element.
(iv) Calculate new circulation from Kutta Joukowski's lift formula in equation (3).
(v) Release vortices into the flow such that total circulation is conserved from the previous time step.
(vi) Propagate all vortices by applying Biot-Savart law.

4. Method

4.1. Benchmark test

Because the CRAFT is a new design, there is no experimental data available for validation of the simulation results. Therefore, as a benchmark test, the current implementation of the vortex method has been used to replicate experimental data from a straight-bladed 12 kW H-rotor VAWT located in Marsta, Uppsala, Sweden, first investigated by Mendoza and Goude[14]. Unlike the vortex method in the previous article, the current vortex method implements a new smoothing function and a maximum value for dynamic stall to increase the stability for the CRAFT simulations. The power coefficient curve and normal forces were reproduced using the current implementation of the vortex method. The normal forces were reproduced for the lowest and the highest TSR values to evaluate performance for both cases. The turbine specification and simulation setup is described in more detail by Mendoza and Goude[14].

4.2. CRAFT simulation

For this study, the CRAFT has been investigated for twenty-one values of TSR, from 4.00 to 9.00 with steps of 0.25. The TSR has been varied by varying the simulated rotational velocity of the CRAFT while free stream velocity has been kept constant $U_\infty = 11$ m/s. For each TSR, the CRAFT has been simulated for tower tilt angles $\varphi = 0°, 15°, 30°, 45°$, to cover all modes of operation and capture the aerodynamic behaviour as the tilt angle is varied.

To allow the wake to stabilize, the simulations were run for 20 revolutions with 120 time steps, which corresponds to azimuth angle of 3° per time step. 28 panel segments were used for the turbine blades and 15 panel segments were used for the struts. The normal force is the resultant of the the radial components of the lift and drag forces from equations (1) and (2). The power coefficient is defined as

$$C_P = \frac{P}{\frac{1}{2} A \rho U_\infty^3}, \tag{4}$$

where P is the average power over one revolution and A is the swept area of the rotor.

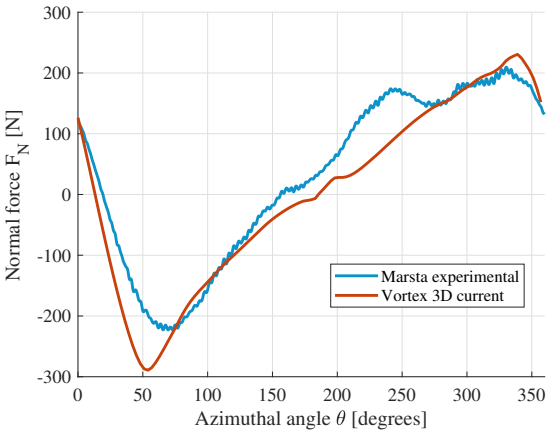

Figure 4: Normal force on blade of 12 kW VAWT during one revolution for TSR 1.84. Experimental data from Mendoza and Goude[14].

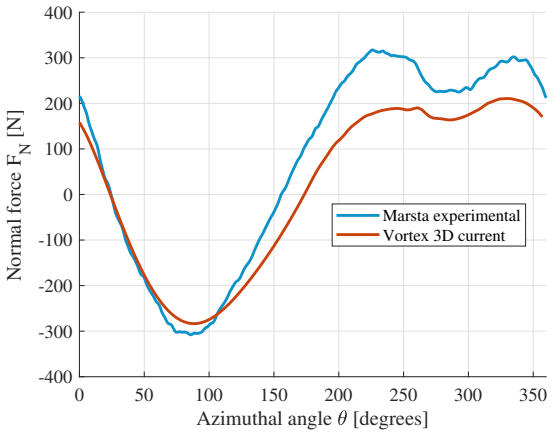

Figure 5: Normal force on blade of 12 kW VAWT during one revolution for TSR 4.57. Experimental data from Mendoza and Goude[14].

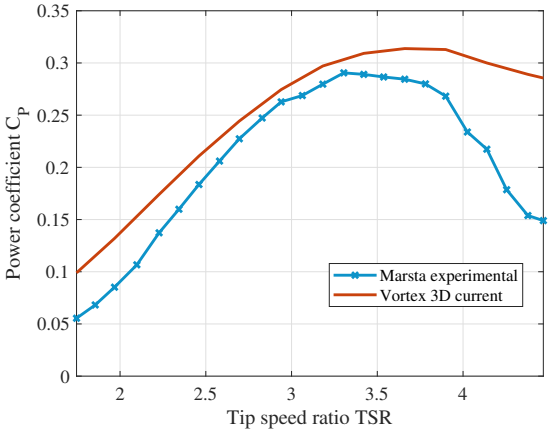

Figure 6: Comparison of power coefficient curves for 12 kW. Experimental data from Mendoza and Goude[14].

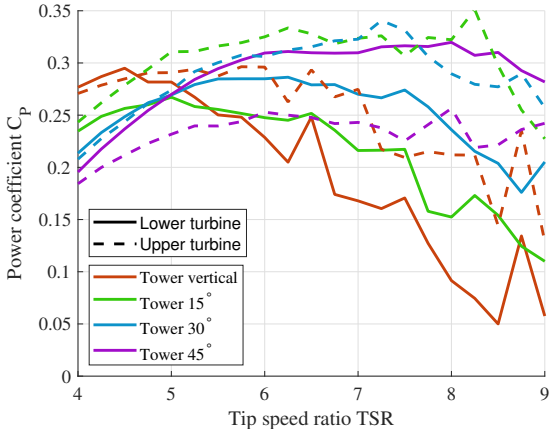

Figure 7: Comparison of power coefficient curves for respective turbine for different tower angles of the CRAFT.

5. Results & Discussion

5.1. Benchmark test results

In figures 4 and 5, the simulated normal forces follow the experimental values for the 12 kW VAWT quite well, both for low and high TSR. In figure 5, the normal force is underestimated during the back sweep of the revolution.

Illustrated in figure 6, the simulation model overestimates C_P, but follows the experimental values quite well for low TSR. However, the C_P does not decrease as expected for higher values of TSR. The underestimation of normal force for high TSR could contribute to this effect. Hence, it seems that the results are more unreliable for higher values of TSR. Overall, the results from the benchmark test shows that the current vortex filament method can be used to simulate the CRAFT with reasonable accuracy.

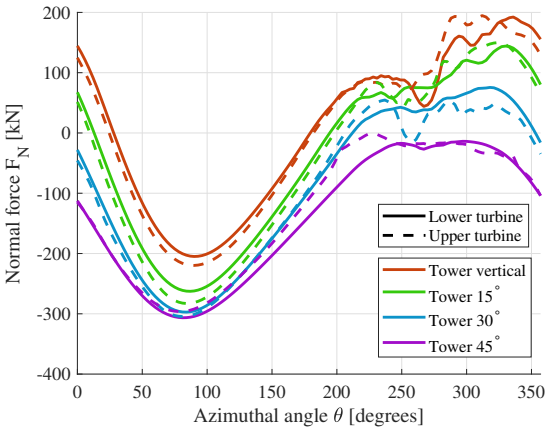

Figure 8: Normal force for a blade during one revolution for different tower angles of the CRAFT.

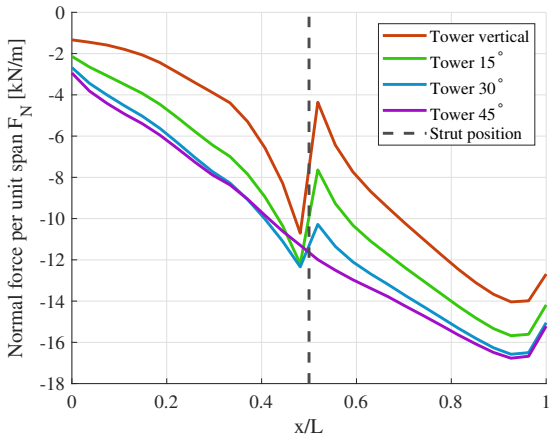

Figure 9: Normal force spanwise along a blade for different tower angles. The blades is located at azimuthal angle $\theta = 90°$.

5.2. Power coefficient plots

Shown in figure 7 are the power coefficient curves for the both turbines. The highest C_P at TSR 6.0 is about 0.33. The upper turbine achieves higher C_P for lower angles and lower C_P for higher angles than the lower turbine. Furthermore, the curves are rougher for the upper turbine compared to the lower turbine. The C_P difference for higher angles is due to the wake from the lower turbine flowing into the upper turbine for higher angles, as can be seen in figure 10.

The power coefficient peak shifts with the tower angle in figure 7; peak values occur for TSR 4.5, 5.5, 6.0 and 6.5 for tower angles 0, 15, 30 and 45, respectively. The CRAFT design should strive to have the peak power production for the desired TSR and angle of operation. Additionally, lower wind speeds means lower thrust force, which consequently lowers tilt. This means that the rotational speed of the turbine must be controlled to account both for the tilt angle and for the wind speed to maintain peak C_P.

5.3. Normal force plots

The normal forces on the blades shown in figure 8 are cyclic, similar to that of the 12 kW VAWT in the benchmark test in section 5.1. The normal force magnitude is similar for both upper and lower turbine throughout the revolution. It is noted that the blade experiences approximately zero normal force during the back sweep when when the tower is tilted 45° and the blade is parallel with the free stream velocity. Furthermore, the peak negative force at $\theta = 90°$ appears to be converging to approximately -300 kN for higher angles. The normal force is expected to be almost constant for 90° tilt angle, because blades would have constant angle of attack and thus constant blade force throughout the revolution. However, since the CRAFT is designed for tilt angles between 0° and 45° , the design must account for cyclical loads on the blades.

It can be observed in figure 9 that there is a sudden change in the normal force along the blade due to the strut. At this point, the strut splits the circulation zone which causes a discontinuity in circulation which is used to calculate the lift coefficient in equations (1) and (3)[15]. There is no discontinuity in the normal force when the tower is tilted 45° because the strut is parallel to the flow and the circulation is not affected. The strut is a known design challenge for VAWTs and is necessary to supply the blade with stability. The normal force along the blade also rises towards the tip of the blade. At the tip, the lift and drag coefficients go to zero, and hence the normal force will also go towards zero at the tip.

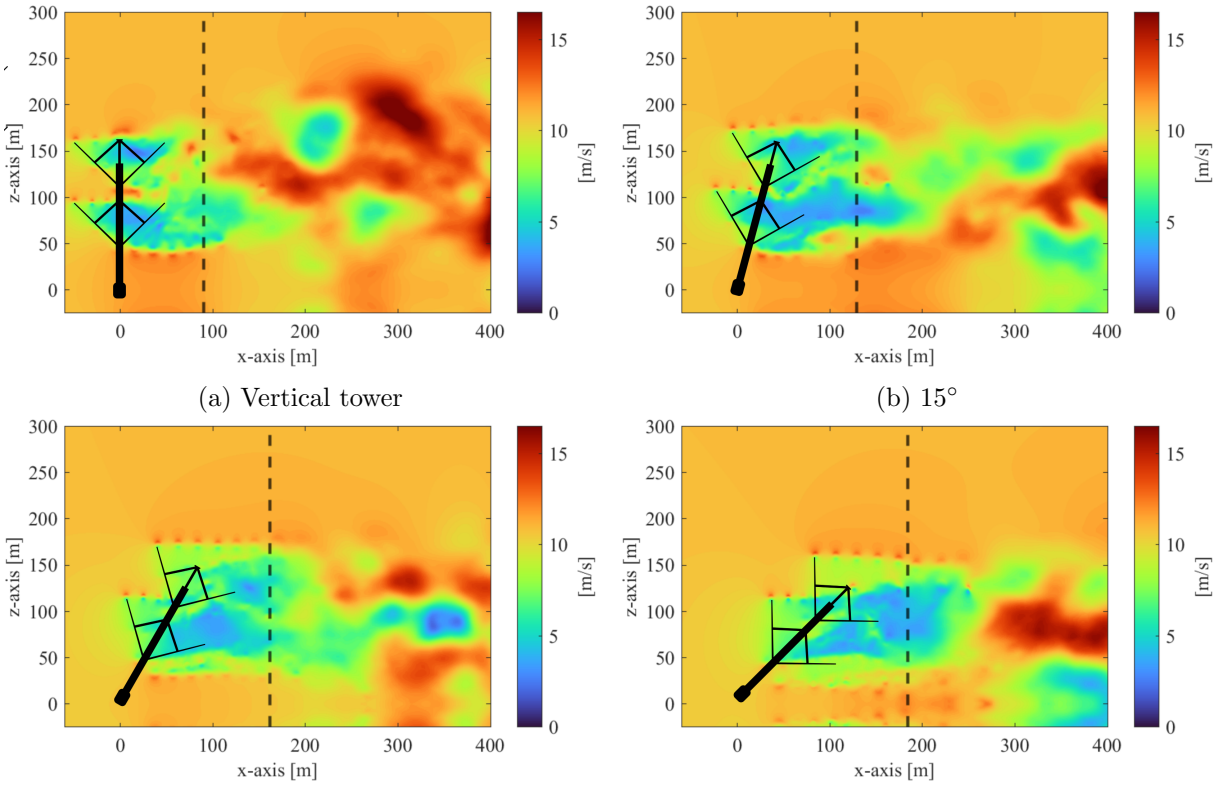

(a) Vertical tower (b) 15°

(c) 30° (d) 45°

Figure 10: Velocity plots xz-plane at $y = 0$ m. The dashed lines are located 25 m downstream from trailing blade tip and represent the yz-planes in figure 11.

5.4. Velocity plots

The velocity plots show the magnitude of the total velocity and illustrates the shape of the wake behind the wind turbine. All velocity plots are produced for TSR 6 and shows the velocity at the final time step of the simulation. In figure 10, it can be seen that the wake is pushed down slightly towards the ground for higher tilt angles. This will cause the wake to interact more with the ground than if the wake flowed horizontally. Here, a flat ground is implemented to account for the ground interaction. In figure 12 a comparison is made between including ground and not including ground. It can be seen that the inclusion of the ground prevents the wake from crossing the $(z = 0)$-plane and affects the wake expansion even near the turbine. However, for in-field application, the water's surface is dynamic. Future studies could investigate the effect of ocean waves on the wake.

Figures 10 and 11 show the wakes from the upper and lower turbines overlapping which is most prominent for 45° tower tilt angle. Wake interaction is an undesired trait for wind turbines due to increase in turbulence which decreases power production, increases noise and unsteady loads[16]. This can be prevented by increasing the spacing between the turbines to account for flow expansion in the wake.

The velocity plots show regions of higher velocity than the free stream velocity. This is not realistic and suggests that the model is prone to some discretization errors. This could be due to distortion of the vortex filaments further downstream as the wake experiences breakdown[17]. Although mass conservation is a condition fulfilled by the model's formulation, the discretization errors introduce problems with conservation of momentum. Due to these errors, simulation results are less viable further downstream.

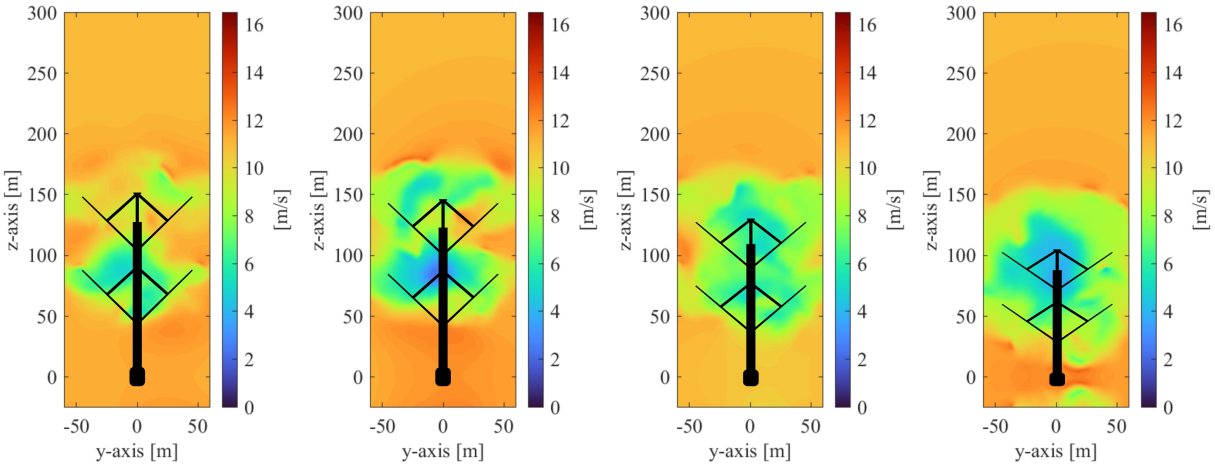

(a) Vertical tower (b) 15° (c) 30° (d) 45°

Figure 11: Velocity plots yz-plane at $x = 25$ m behind the turbine trailing blade tip.

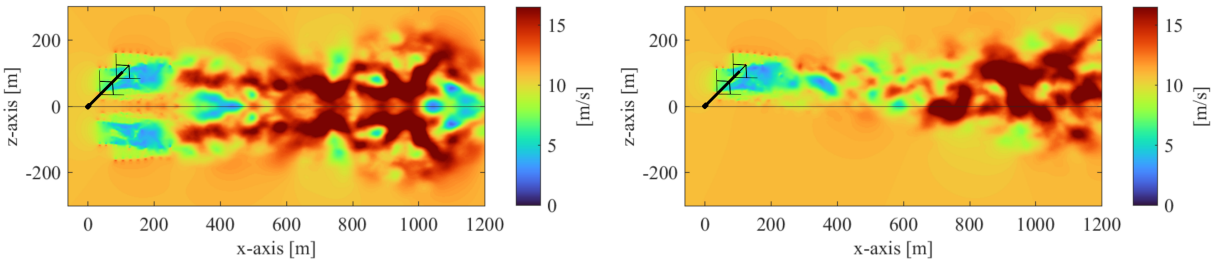

(a) Ground included (b) Ground not included

Figure 12: Comparison between including and not including a flat ground in the simulations for a CRAFT that's tilted 45°.

6. Conclusions

The CRAFT is a new wind turbine design for floating off-shore wind power that includes two counter-rotating turbines and allows for the tower to tilt. The CRAFT has been simulated using a 3D vortex filament method to study the effect of the tower tilt angle on the power coefficient and normal forces for multiple TSRs.

The current 3D vortex filament method implementation was validated using a benchmark test. The simulation results proved sufficiently accurate to simulate the CRAFT's performance and normal forces. However, regions of high velocity were observed in the wake due to wake breakdown. Hence, the current implementation is not suited for wake studies far downstream. Further validation could be performed using other simulation methods such as the actuator line model with Large Eddy Simulation (LES) on a traditional mesh. Additionally, if a pilot CRAFT is built, the simulation results could be validated against experimental data.

The peak C_P was observed to shift with the tower angle, and the design should therefore ensure that the tower tilt angle is optimal during rated operation. Higher values for C_P are expected from optimization of the CRAFT. For example, a more suitable wing profile than the NACA0021 could be found. Additionally, a proper method for determining the C_P with varying tower tilt angle is crucial.

The normal forces on the CRAFT's blades fluctuate, proposing similar structural challenges as to VAWTs. However, in contrast to the VAWT, the normal force amplitude varies with the

CRAFT's tower tilt angle. Therefore, when designing the CRAFT, the blades must be designed to withstand the maximum normal force and force fluctuations for all tower tilt angles.

The velocity plots illustrate the wake flow of the CRAFT. The plots show that the wakes from the lower and upper turbines interact for high tilt angles. This can be avoided by increasing the spacing between the turbines. The velocity plots also show the CRAFT's wake being pushed slightly towards the ground. The wake will therefore be more likely to interact with the water's surface. Therefore, it would be of interest to investigate the wake with a dynamic ground and a non-constant wind profile.

For future work, more design parameters could be investigated, such as the spacing between the turbines or the angle of the V-shape of the turbine blades. Furthermore, choice of wing profiles for blades and struts and pitch angle could be investigated for optimal energy production.

This study serves as a basis for further development and pilot testing for the CRAFT. Several aspects of the CRAFT can be investigated further. The results show that there are plenty of opportunities of improvement for the design investigated in this simulation study. In conclusion, the results give insight into the aerodynamic behaviour of the CRAFT which enables further development.

References

[1] E. P. Soares-Ramos, L. de Oliveira-Assis, R. Sarrias-Mena, and L. M. Fernández-Ramírez, "Current status and future trends of offshore wind power in europe," *Energy*, vol. 202, p. 117787, 2020.
[2] "Norway announces big new offshore wind targets." `https://windeurope.org/newsroom/news/norway-announces-big-new-offshore-wind-targets/`. Accessed: 2023-02-27.
[3] R. Perveen, N. Kishor, and S. R. Mohanty, "Off-shore wind farm development: Present status and challenges," *Renew. and Sust. Energy Reviews*, vol. 29, pp. 780–792, 2014.
[4] N. A. Ahmed and M. Cameron, "The challenges and possible solutions of horizontal axis wind turbines as a clean energy solution for the future," *Renew. and Sust. Energy Reviews*, vol. 38, pp. 439–460, 2014.
[5] A. Arredondo-Galeana and F. Brennan, "Floating offshore vertical axis wind turbines: Opportunities, challenges and way forward," *Energies*, vol. 14, no. 23, 2021.
[6] "Next generation floating off-shore wind." `https://worldwidewind.no/`. Accessed: 2023-02-27.
[7] I. M. Solbrekke and A. Sorteberg, "Nora3-wp: A high-resolution offshore wind power dataset for the baltic, north, norwegian, and barents seas," *Scientific Data*, vol. 9, no. 1, p. 362, 2022.
[8] W. R. Skrzypiński, J. I. Bech, C. B. Hasager, A.-M. Tilg, and F. V. C. Bak, "Optimization of the erosion-safe operation of the iea wind 15 mw reference wind turbine," *J. of Physics: Conference Series*, vol. 1618, p. 052034, sep 2020.
[9] D. Holst, B. Church, F. Wegner, G. Pechlivanoglou, C. N. Nayeri, and C. O. Paschereit, "Experimental Analysis of a NACA 0021 Airfoil Under Dynamic Angle of Attack Variation and Low Reynolds Numbers," *J. of Eng. Gas Turbines Power*, vol. Volume 9: Oil and Gas Applications; Supercritical CO2 Power Cycles; Wind Energy, 06 2018. V009T48A010.
[10] S. B. Qamar and I. Janajreh, "Numerical investigation of solidity for cambered darrieus vawts: Analysis of chord length," in *2016 International Renew. and Sust. Energy Conference (IRSEC)*, pp. 901–905, IEEE, Nov. 2016.
[11] A. Leonard, "Vortex methods for flow simulation," *J. of Comp. Physics*, vol. 37, no. 3, pp. 289–335, 1980.
[12] E. Dyachuk, A. Goude, and H. Berhnoff, "Simulating Pitching Blade With Free Vortex Model Coupled With Dynamic Stall Model for Conditions of Straight Bladed Vertical Axis Turbines," *J. of Solar Energy Engineering*, vol. 137, 08 2015. 041008.
[13] E. Dyachuk and A. Goude, "Numerical validation of a vortex model against experimental data on a straight-bladed vertical axis wind turbine," *Energies*, vol. 8, no. 10, pp. 11800–11820, 2015.
[14] V. Mendoza and A. Goude, "Validation of actuator line and vortex models using normal forces measurements of a straight-bladed vertical axis wind turbine," *Energies*, vol. 13, no. 3, 2020.
[15] A. Aihara, V. Mendoza, A. Goude, and H. Bernhoff, "Comparison of three-dimensional numerical methods for modeling of strut effect on the performance of a vertical axis wind turbine," *Energies*, vol. 15, no. 7, 2022.
[16] J. F. Manwell, *Wind energy explained : theory, design and application*. Chichester: Wiley, 2. ed. ed., 2009.
[17] M. Carrión, M. Woodgate, R. Steijl, G. N. Barakos, S. Gomez-Iradi, and X. Munduate, "Understanding wind-turbine wake breakdown using computational fluid dynamics," *AIAA Journal*, vol. 53, no. 3, pp. 588–602, 2015.